HOXA5-induced lncRNA *DNM3OS* promotes human embryo lung fibroblast fibrosis via recruiting EZH2 to epigenetically suppress *TSC2* expression

Hong Lv[#], Xingjia Qian[#], Zhengzheng Tao, Jun Shu, Dongfang Shi, Jing Yu, Guiqin Fan, Qiuhong Qian, Luhong Shen, Bing Lu

Department of Pulmonary and Critical Care Medicine, Taicang TCM Hospital, Affiliated to Nanjing University of Chinese Medicine, Taicang, China
Contributions: (I) Conception and design: H Lv, X Qian; (II) Administrative support: Z Tao, J Shu; (III) Provision of study materials or patients: D Shi, J Yu, G Fan; (IV) Collection and assembly of data: Q Qian, L Shen; (V) Data analysis and interpretation: B Lu; (VI) Manuscript writing: All authors; (VII) Final approval of manuscript: All authors.
[#]These authors contributed equally to this work.
Correspondence to: Bing Lu, BS. Department of Pulmonary and Critical Care Medicine, Taicang TCM Hospital, Affiliated to Nanjing University of Chinese Medicine, No. 140, South Renmin Road, Taicang 215499, China. Email: tczyyLb@163.com.

Background: Idiopathic pulmonary fibrosis (IPF) is an unrepairable disease that results in lung dysfunction and decreased quality of life. Prevention of pulmonary fibrosis is challenging, while its pathogenesis remains largely unknown. Herein, we investigated the effect and mechanism of long non-coding RNA (lncRNA) *DNM3OS*/Antisense RNA in the pathogenesis of pulmonary fibrosis.

Methods: EdU (5-ethynyl-2'-deoxyuridine) and wound healing assays were employed to evaluate the role of DNM3OS on cell proliferation and migration. Western blot detected the proteins expressions of alpha-smooth muscle actin (α-SMA), vimentin, and fibronectin. The interactions among genes were evaluated by RNA pull-down, luciferase reporter, RNA immunoprecipitation (RIP), chromatin immunoprecipitation (ChIP) and chromatin Isolation by RNA purification (ChIRP) assays.

Results: *DNM3OS* was upregulated by transforming growth factor beta 1 (TGF-β1) in a dose- and time-dependent manner. *DNM3OS* knockdown repressed the growth and migration of lung fibroblast, and fibrotic gene expression (*CoL1α1*, *CoL3α1*, α-SMA, vimentin, and fibronectin), while suppression of *TSC2* accelerated the above process. DNM3OS recruited EZH2 to the promoter region of *TSC2*, increased the occupancy of EZH2 and H3K27me3, and thereby suppressed the expression of *TSC2*. *HOXA5* promoted the transcription of *DNM3OS*.

Conclusions: *HOXA5*-induced *DNM3OS* promoted the proliferation, migration, and expression of fibrosis-related genes in human embryo lung fibroblast via recruiting EZH2 to epigenetically suppress the expression of *TSC2*.

Keywords: Idiopathic pulmonary fibrosis (IPF); long noncoding RNA *DNM3OS* (lncRNA *DNM3OS*); *HOXA5*; *TSC2*; *EZH2*

Introduction

The cause that leads to chronic and progressive interstitial lung disease (ILD) and idiopathic pulmonary fibrosis (IPF) remains unidentified (1,2). The incidence of IPF ranges from 2.8 to 9.3 cases per 100,000 people annually in North America and Europe, higher than that in other regions (3). IPF usually occurs in elderly people and is often misdiagnosed and inappropriately treated, which leads to

high mortality rate (1). Epithelial injury and subsequent aberrant repair of injury cells, along with senescence of alveolar epithelial cells, may lead to lung fibrosis (1,2). Mediators for IPF include shortened telomeres, oxidative stress, endoplasmic reticulum stress, and mitochondrial dysfunction (4,5). In addition, the immune system also contributes to the development of IPF (6). Although some medications are available to slow down the progression of IPF (7), it is impossible to prevent the occurrence or reverse IPF. Thus, it is important to understand the pathogenesis of and explore the novel therapeutic target for clinical management of IPF.

Transcription factors (TFs) are a group of evolution-conserved DNA binding proteins that master gene transcription (8). TFs specifically recognize and bind to short DNA motifs, followed by recruiting transcription machinery to regulate gene transcription (8). Some TFs are tissue- and cell type-specific and thus participate in maintaining tissue homeostasis and disease pathogenesis. The involvement of TFs in IPF development is well documented (9). For example, Lin *et al.* reported the role of runt-related transcription factor 1 (*RUNX1*) in promoting IPF (9). The level of transcription factor *RUNX2* is also upregulated in fibrotic lung and associated with disease severity (10), whereas transcription factor Yin Yang 1 (*YY1*) inhibits the expression of Thymocyte differentiation antigen-1 (*THY1*) to aggravate IPF (11). Epithelial-

mesenchymal transition (EMT) also promotes lung fibrosis progression (12). A previous study reported the increased activity of Axl to facilitate the development of IPF (13), while loss of Axl resulted in EMT transcription factors including snail family transcriptional repressor 2 (*SNAI2*), *HOXA5*, T-Box transcription factor 2 or 3 (*TBX2* or *TBX3*) (14). Therefore, we supposed that *HOXA5* may possess a yet unknown function in IPF. However, the underlying mechanism remains incompletely investigated.

Long non-coding RNA (lncRNA) is non-protein coding RNA with more than 200 nucleotides in length that participates in gene imprinting, differentiation and development, and disease (15,16). Many studies interrogating the pathogenesis of IPF have found many diseases related to lncRNAs. LncRNA has been implicated in the regulation of transforming growth factor beta 1 (TGF-β1) (17). LncRNA Airn alleviate liver fibrosis via the Kruppel-like factor 2 (KLF2)-endothelial nitric oxide synthase (eNOS)-soluble guanylate cyclase (sGC) pathway (18), while Zinc finger E-box binding homeobox 1 antisense 1 (*ZEB1-AS1*) contributes to lung fibrosis by facilitating EMT (19). LncRNA *DNM3OS* is induced by TGF-β1 which results in the production of profibrotic microRNAs (miRNAs) (20), and targeting *DNM3OS* shows promising therapeutic effects in fibroproliferative diseases including IPF (21). As a critical regulator for IPF, the underlying molecular mechanism of *DNM3OS* in IPF pathogenesis remains elusive.

Both *HOXA5* and lncRNA *DNM3OS* are regulated by TGF-β signaling, but their relationship is unknown, particularly in the context of lung fibrosis. Therefore, we hypothesized that *HOXA5*-induced *lncRNA DNM3OS* promoted the proliferation, migration, and expression of fibrosis-related genes in human embryo lung fibroblast by recruiting EZH2 to inhibit *TSC2* expression. Here, we elucidated the molecular mechanism through which *DNM3OS* promotes lung fibrosis and highlighted the potential of targeting *DNM3OS* in anti-fibrotic therapy. We present this article in accordance with the MDAR reporting checklist (available at https://jtd.amegroups.com/article/view/10.21037/jtd-23-1145/rc).

Highlight box

Key findings

• *HOXA5*-induced *DNM3OS* promoted the proliferation, migration, and the expression of fibrosis-related genes in human embryo lung fibroblast via recruiting EZH2 to epigenetically suppress the expression of *TSC2*.

What is known and what is new?

• *DNM3OS* and *HOXA5* are upregulated by TGF-β1 to promote fibrosis.

• *HOXA5* promotes the transcription of *DNM3OS*, which recruits EZH2 to the promoter region of *TSC2*, increased the occupancy of EZH2 and H3K27me3, resulting in the enhanced proliferation, migration and expression of fibrosis-related genes in human embryo lung fibroblast.

What is the implication, and what should change now?

• This study elaborates the mechanisms of *HOXA5*-induced *DNM3OS* in fibrosis through recruiting EZH2 to epigenetically suppress *TSC2* expression. Targeting this axis holds great potential to treat lung fibrosis.

Methods

Clinical samples

Blood from 10 healthy controls (age: 62–76 years, 50% male) and 8 patients with IPF (age: 65–80 years, 50% male) was collected. All patients were reviewed for the current study

to validate the diagnosis of IPF according to the American Thoracic Society (ATS)/European Respiratory Society (ERS)/Japanese Respiratory Society (JRS)/Latin American Thoracic Society (ALAT) criteria (22). Other forms of interstitial pneumonia including other idiopathic ILD and ILD associated with systemic disease, environmental, exposure or medication were excluded. In addition, patients with chronic hypersensitivity pneumonitis as a hidden cause of IPF was also excluded. The high-resolution computed tomography and laboratory examination were also exploited to exclude connective tissue disease (23). All cases were evaluated by a multidisciplinary group composed of a pulmonologist, a specialist in pulmonary rehabilitation, a rheumatologist, a radiologist, a pathologist and a specialist in occupational medicine. Samples were stored at –80 ℃ until analyses. This study was conducted in accordance with the Declaration of Helsinki (as revised in 2013). The study was approved by Taicang TCM Hospital, Affiliated to Nanjing University of Chinese Medicine (No. 2023024). Written informed consent was obtained from each participant in this study.

Cell culture

Human embryo lung fibroblast (HELF) [#PCS-201-013, American type culture collection (ATCC)] and WI-38 (#CCL-75, ATCC) were maintained in Dulbecco's modified Eagle medium (DMEM, Cat. #12430054, Gibco, Waltham, MA, USA) with 10% fetal bovine serum (FBS, #26140079, Gibco), 1% Penicillin-Streptomycin (#15140122, Gibco) in incubator with 5% CO_2 at 37 ℃.

Plasmid construction and cell transfection

DNM3OS-, EZH2- and *TSC2*-targeting short hairpin RNA (shRNA) were cloned into pLKO.1-puro vector (Addgene, Cambridge, MA, USA). *HOXA5* open reading frame region was cloned and inserted into pcDNA3.1 vector (Addgene). The promoter region of LncRNA *DNM3OS* was cloned into pGL4 luciferase reporter vector (Promega, Madison, WI, USA). Lung fibroblasts were cultured in 6-well plates overnight before transfection with lipofectamine 2000. Cells were cultured for 48 h before further analysis.

Cell proliferation assay

Cell growth was evaluated using EdU (5-ethynyl-2'-deoxyuridine) staining proliferation kit (#ab22421, Abcam,

Cambridge, UK). Cells at 60–70% confluency were cultured with EdU for 4 h before fixation in 4% formaldehyde and permeabilization. EdU reaction mix was incubated with cells in dark. After staining of the nucleus with Hoechst 33342, cells were examined and imaged by fluorescence microscope.

Wound healing assay

After 18–24 h culture, the confluent cells were scraped with a 1 mm pipette tip, followed by three times wash with phosphate buffered saline (PBS) and replenished with 2 mL complete medium. The cells were imaged immediately as well as 48 h later under microscope.

RNA isolation, reverse transcription polymerase chain reaction (PCR), and quantitative reverse transcription PCR (qRT-PCR)

Total RNA isolation and reverse transcription were performed using the RNeasy Mini Kit (#74104, QIAGEN, New York, NY, USA) and the High-Capacity cDNA Reverse Transcription Kit (#4368814, Applied Biosystems, Waltham, MA, USA), respectively. The SsoAdvanced Universal SYBR Green Supermix (#1725270, BIO-RAD, Hercules, CA, USA) was used for quantitative PCR (qPCR). Glyceraldehyde phosphate dehydrogenase (GAPDH) was used as reference gene. The primers for the tested genes are listed below.

DNM3OS-F: 5'-GGTCCTAAATTCATTGCCAGTTC-3',
DNM3OS-R: 5'-ACTCAAGGGCTGTGATTTCC-3';
CoL1α1-F: 5'-GAGGGCCAAGACGAAGACATC-3',
CoL1α1-R: 5'-CAGATCACGTCATCGCACAAC-3';
CoL3α1-F: 5'-TTGAAGGAGGATGTTCCCATCT-3',
CoL3α1-R: 5'-ACAGACACATATTTGGCATGGTT-3';
TSC2-F: 5'-CTCCCATCCAGTCCTGCTAC-3',
TSC2-R: 5'-TCACTCACCTTGATGGTGCC-3';
U6-F: 5'-CTCGCTTCGGCAGCACA-3',
U6-R: 5'-AACGCTTCACGAATTTGCGT-3';
GAPDH-F: 5'-*TGATTCTACCCACGGCAAGTT*-3',
GAPDH-R: 5'-TGATGGGTTTCCCATTGATGA-3'.

Western blot analysis

Proteins were extracted in radio immunoprecipitation assay (RIPA) buffer and were electrophoresed in 12% sodium dodecyl sulphate-polyacrylamide gel electrophoresis (SDS-PAGE) and transferred onto a polyvinylidene difluoride membrane. After blocking in 5% TBST buffer, the

membrane was incubated overnight at 4 ℃ with the primary antibody, and the horseradish peroxidase-conjugated secondary antibodies, the blots were developed with enhanced chemiluminescence (ECL) kits (#1705060S, BIO-RAD). Images were captured by a ChemicDoc XRS system (Bio-Rad). Antibodies used were anti-α-SMA (Cat. #14968, CST, Boston, MA, USA), anti-vimentin (Cat. #5741, CST), anti-fibronectin (Cat. #26836, CST), anti-EZH2 (Cat. #5246, CST), anti-TSC2 (Cat. #3612, CST), anti-GAPDH (Cat. #5174, CST).

RNA immunoprecipitation (RIP)

RIP was performed following the previous protocol (24). Briefly, cell lysis was incubated with EZH2 antibody-conjugated magnetic beads. After extensive washes and treatment with proteinase K, RNA was extracted by phenol:chloroform: isoamyl alcohol solution, dissolved in RNase-free H_2O and detected by PCR. A random sequence was used as negative control for RIP.

RNA pull-down

The process for RNA pull-down had been described previously (25). Cells were homogenized in hypotonic buffer and incubated with biotinylated DNM3OS or control antisense RNA-conjugated beads with RNase inhibitor. After extensive washes, RNA-binding proteins were dissolved in Laemmli buffer and examined by Western blotting assay. A random sequence was used as negative control for RIP.

Chromatin immunoprecipitation (ChIP)

Formaldehyde-mediated crosslinking of protein-DNA complexes was quenched by glycine. Cells lysis was sonicated and centrifuged to collect the supernatant, which was incubated with biotinylated EZH2 and α-HOXA5 antibody. Streptavidin beads were used to enrich the chromatin-protein complex, followed by DNA extraction. The promoter of TSC2 and DNM3OS was checked by PCR. A random sequence was used as negative control, while MAX dimerization protein 1 (MXD1) promoter was used as a positive control (26).

Chromatin isolation by RNA purification (ChIRP)

ChIRP assay was performed with a Magna ChIRP Kit (Sigma-Aldrich, St. Louis, MO, USA). Cell lysate was ultrasonicated and centrifugated, the supernatant was incubated with probes and complete hybridization buffer for 4 h at 37 ℃. The cocktail mixed with streptavidin magnetic beads was washed for five times. Finally, qPCR/qRT-PCR were performed to detect the interaction between lncRNA DNM3OS and TSC2 promoter.

Luciferase assay

Luciferase activity was evaluated by the luciferase assay kit (#E1500, Promega). Cells co-transfected DNM3OS luciferase reporter with vector or HOXA5 expressing plasmid were cultured for 48 h in 96-well plates. Twenty microliter of lysis reagent was added into each well and then mixed with 100 μL of Luciferase Assay Reagent. The luminescence intensity was recorded withGloMax 96 Luminometer (Progema).

Statistical analysis

Experiment was performed for at least three times. Data were shown as mean ± standard deviation (SD). One-way Analysis of Variance (ANOVA) or Student's t-test was used for statistical analysis with a SPSS software (SPSS Inc., Chicago, IL, USA). $P<0.05$ was considered statistically significant.

Results

TGF-β1 upregulated lncRNA DNM3OS expression in lung fibroblast

A prior study has reported that the involvement of lncRNA DNM3OS in pulmonary fibrosis (20). We collected blood from 8 patients with IPF and 10 healthy controls and examined the expression of lncRNA DNM3OS. The levels of lncRNA DNM3OS were significantly higher in IPF patients than those in healthy individuals (Figure S1A). To assess the effect of TGF-β1 on lncRNA DNM3OS expression in lung fibroblast, HELF and WI-38 cells were cultured in gradually increased concentration of TGF-β1. The level of DNM3OS was elevated along with increased TGF-β1 and increased to about 3-fold with 10 ng/ml TGF-β1, compared to untreated cells (Figure 1A). Besides, TGF-β1 upregulated DNM3OS in a time-dependent manner. TGF-β1 did not cause significant change of DNM3OS at 3 h, while DNM3OS expression was significantly upregulated
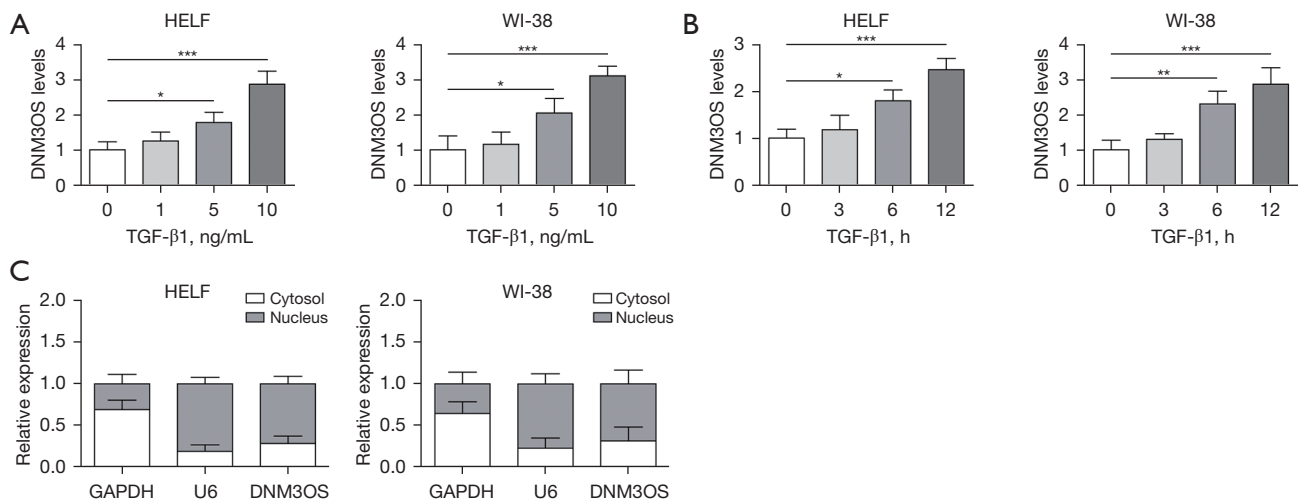
Figure 1 TGF-β1 upregulated *lncRNA DNM3OS* expression in lung fibroblast. (A) Lung fibroblast HELF and WI-38 were treated with indicated concentration of TGF-β1. LncRNA *DNM3OS* level was evaluated by qRT-PCR. (B) After treatment with TGF-β1 for indicated time, lncRNA *DNM3OS* level was assessed by qRT-PCR in HELF and WI-38. (C) HELF and WI-38 cells were subjected to nucleus and cytosol fractionation, and the levels of *DNM3OS* in the nucleus and cytosol were evaluated by qRT-PCR. *, P<0.05; **, P<0.01; ***, P<0.001. LncRNA, long noncoding RNA; HELF, human embryo lung fibroblast; TGF-β1, transforming growth factor beta 1; qRT-PCR, quantitative reverse transcription real-time polymerase chain reaction; GAPDH, glyceraldehyde phosphate dehydrogenase.

at 6 h and 12 h post TGF-β1 treatment (*Figure 1B*). Cytosol-nucleus fractionation showed that DNM3OS was mainly localized in the nuclear localization (*Figure 1C*). These data demonstrated that TGF-β1 induced lncRNA *DNM3OS* expression in lung fibroblasts.

HOXA5 promoted the transcription of DNM3OS

JASPAR-based bioinformatics analysis discovered that there was a potential *HOXA5* binding motif in *DNM3OS* promoter (*Figure 2A*). The DNM3OS-WT increased the luciferase activity, while cells expressing scramble vector or DNM3OS-MUT didn't show an elevation of luciferase activity after *HOXA5* overexpression, which indicated *HOXA5* enhanced activation of *DNM3OS* promoter (*Figure 2B*). A prior study reported the interaction between *MXD1* and *HOXA5* (26). Our ChIP results showed that *HOXA5* antibody enriched a large amount of *MXD1* and *DNM3OS*, but not the scramble control, while Immunoglobulin G (IgG) control failed to pull down any targets examined (*Figure 2C*). Overexpression of *HOXA5* in HELF cells significantly increased *DNM3OS* expression (*Figure 2D*). These data demonstrated that *HOXA5* bound to the promoter of *DNM3OS* and thus promoted its transcription.

Loss of DNM3OS attenuated proliferation and the expression of fibrosis-related genes

Among the three *DNM3OS*-targeting shRNAs, sh-DNM3OS-2 and sh-DNM3OS-3 effectively downregulated the expression of *lncRNA DNM3OS* in HELF and WI-38 cells (*Figure 3A*). Therefore, sh-DNM3OS-2 and sh-DNM3OS-3 were used for subsequent experiments. TGF-β1 treatment promoted proliferation of HELF and WI-38 cells, while the proliferative activity of TGF-β1 was diminished in cells with *DNM3OS* knockdown (*Figure 3B*). TGF-β1 promoted migration of lung fibroblasts, but the migratory ability of HELF and WI-38 cells was suppressed by *DNM3OS* knockdown (*Figure 3C*). The expression of alpha 1 type I collagen (*CoL1α1*) and alpha 1 type III collagen (*CoL3α1*) in HELF and WI-38 cells were induced by TGF-β1, while suppressing of *DNM3OS* attenuated TGF-β1-induced *CoL1α1* and *CoL3α1* expression (*Figure 3D*). Moreover, TGF-β1-induced expression of α-SMA, vimentin, and fibronectin was inhibited in lung fibroblast by sh-DNM3OS-2 and sh-DNM3OS-3 (*Figure 3E*). Together, these data demonstrated that loss of *DNM3OS* attenuated the pro-proliferative and pro-fibrotic activity of TGF-β1 in lung fibroblasts.
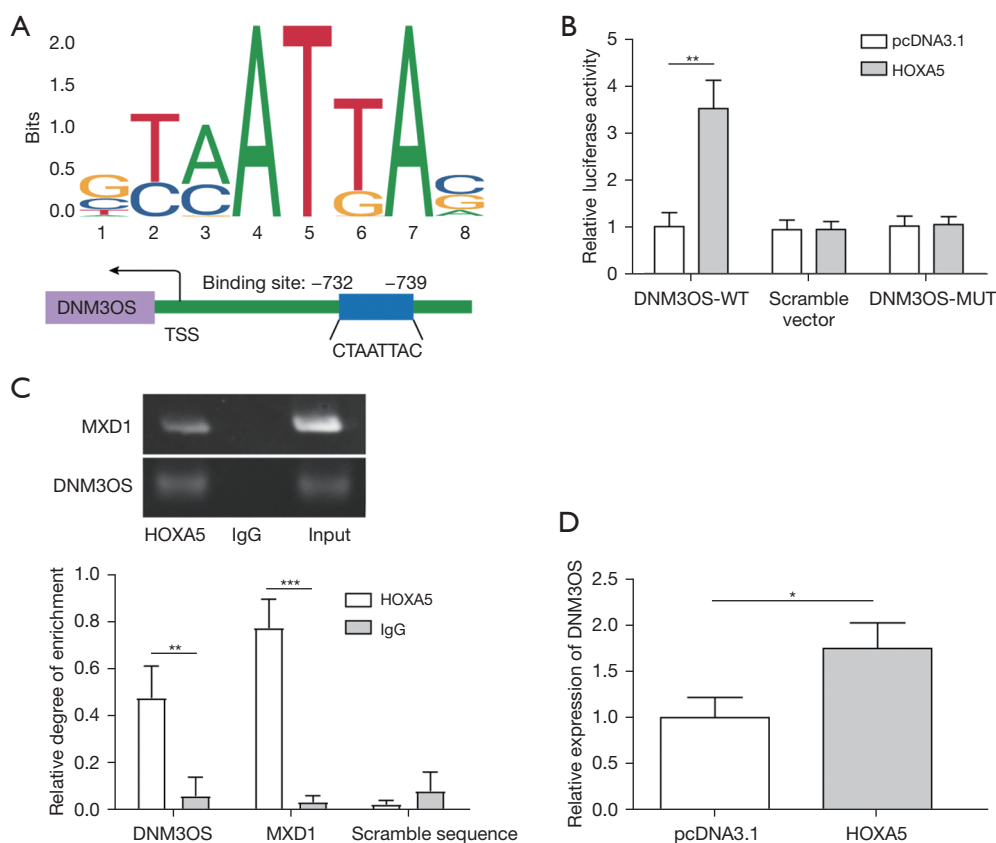
Figure 2 *HOXA5* promoted the transcription of *DNM3OS*. (A) Potential *HOXA5* binding site in the promoter of *DNM3OS* predicted by JASPAR database. (B) *DNM3OS* promoter luciferase reporter expressing HELF cells were transfected with pcDNA3.1 or *HOXA5* plasmid, and luciferase activity was determined by dual-luciferase assay. (C) ChIP was performed to confirm the relationship between *DNM3OS* and *HOXA5*. The promoter of *DNM3OS* was amplified by PCR and the level was determined by agarose electrophoresis. (D) *DNM3OS* level in HELF cells transfected with pcDNA3.1 or HOXA5 plasmid was determined by qRT-PCR. *, P<0.05; **, P<0.01; ***, P<0.001. HELF, human embryo lung fibroblast; pcDNA3.1, the control plasmid; ChIP, chromatin immunoprecipitation; PCR, polymerase chain reaction; qRT-PCR, quantitative reverse transcription real-time polymerase chain reaction; IgG, immunoglobulin G; TSS, transcription start site; WT, wide type; MUT, mutant.

LncRNA DNM3OS suppressed the expression of TSC2 through recruiting EZH2

Subsequently, we further explored the underlying mechanism of *DNM3OS* mediated proliferation and the expression of fibrosis-related genes in lung fibroblast. RIP assay revealed that EZH2 specifically bound to *DNM3OS* but not the scramble control, the IgG control didn't bind to *DNM3OS* or the scramble control (*Figure 4A*). RNA pull-down assay validated that the interaction between *DNM3OS* and EZH2, while the antisense or scramble controls failed to pull down EZH2 in HELF and WI-38

cells (*Figure 4B*). In sh-DNM3OS expressing HELF and WI-38 cells, the levels of *TSC2* were dramatically elevated (*Figure 4C,4D*). In the absence of *DNM3OS*, occupancy of EZH2 and H3K27me3 in the promoter region of *TSC2* was reduced (*Figure 4E*). ChIRP assay verified the interaction between *DNM3OS* and *TSC2* (Figure S1B,1C). Consistently, knockdown of EZH2 also resulted in elevation of *TSC2* expression at mRNA and protein level (*Figure 4F,4G*). These data collectively demonstrated that *lncRNA DNM3OS* directly interacted with EZH2 and prevented its binding to the promoter region of *TSC2*, thus inhibiting its expression.
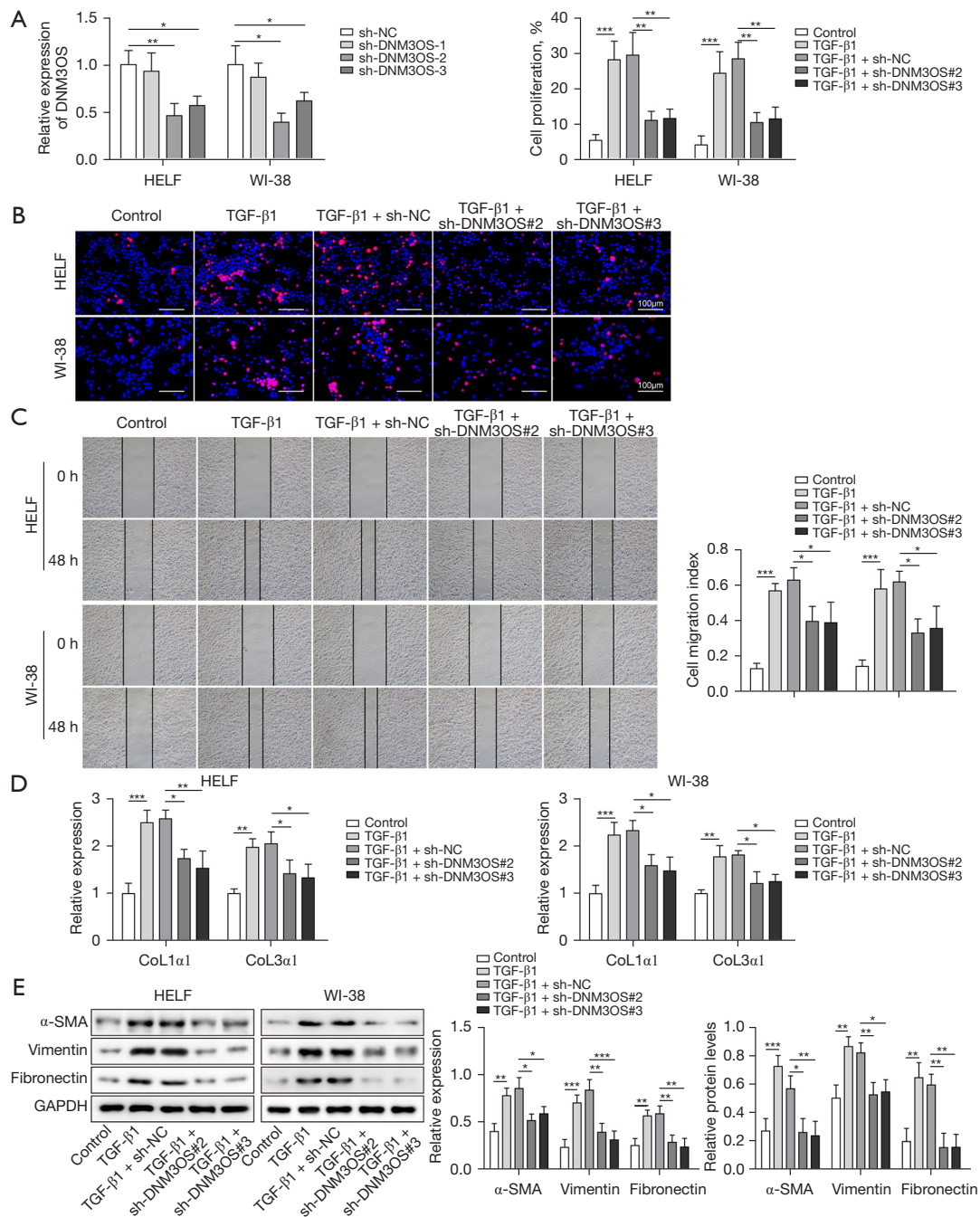
Figure 3 Loss of *DNM3OS* attenuated growth and the expression of fibrosis-related genes. (A) The level of *DNM3OS* in HELF and WI-38 cells expression sh-NC and sh-DNM3OS were evaluated by qRT-PCR. (B-E) WT and shRNA expressing lung fibroblasts were challenged with vehicle control or TGF-β1. The proliferation (B) and migration activity (C) of HELF and WI-38 cells were examined by EdU and wound healing assay, respectively. For EdU assay, the EdU probe was conjugated with a fluorescent dye, and the nucleus was stained by Hoechst 33342 and was examined under a fluorescent microscope. *CoL1α1* and *CoL3α1* expression (D) in HELF and WI-38 cell was assessed by qRT-PCR. The levels of α-SMA, vimentin, and fibronectin (E) in HELF and WI-38 cell were evaluated by western blot. *, P<0.05; **, P<0.01; ***, P<0.001. HELF, human embryo lung fibroblast; qRT-PCR, quantitative reverse transcription real-time polymerase chain reaction; WT, wide type; TGF-β1, transforming growth factor beta 1; shRNA, short hairpin RNA; sh-NC, short hairpin RNA negative control; EdU, 5-ethynyl-2'-deoxyuridine; α-SMA, alpha-smooth muscle actin; GAPDH, glyceraldehyde phosphate dehydrogenase.
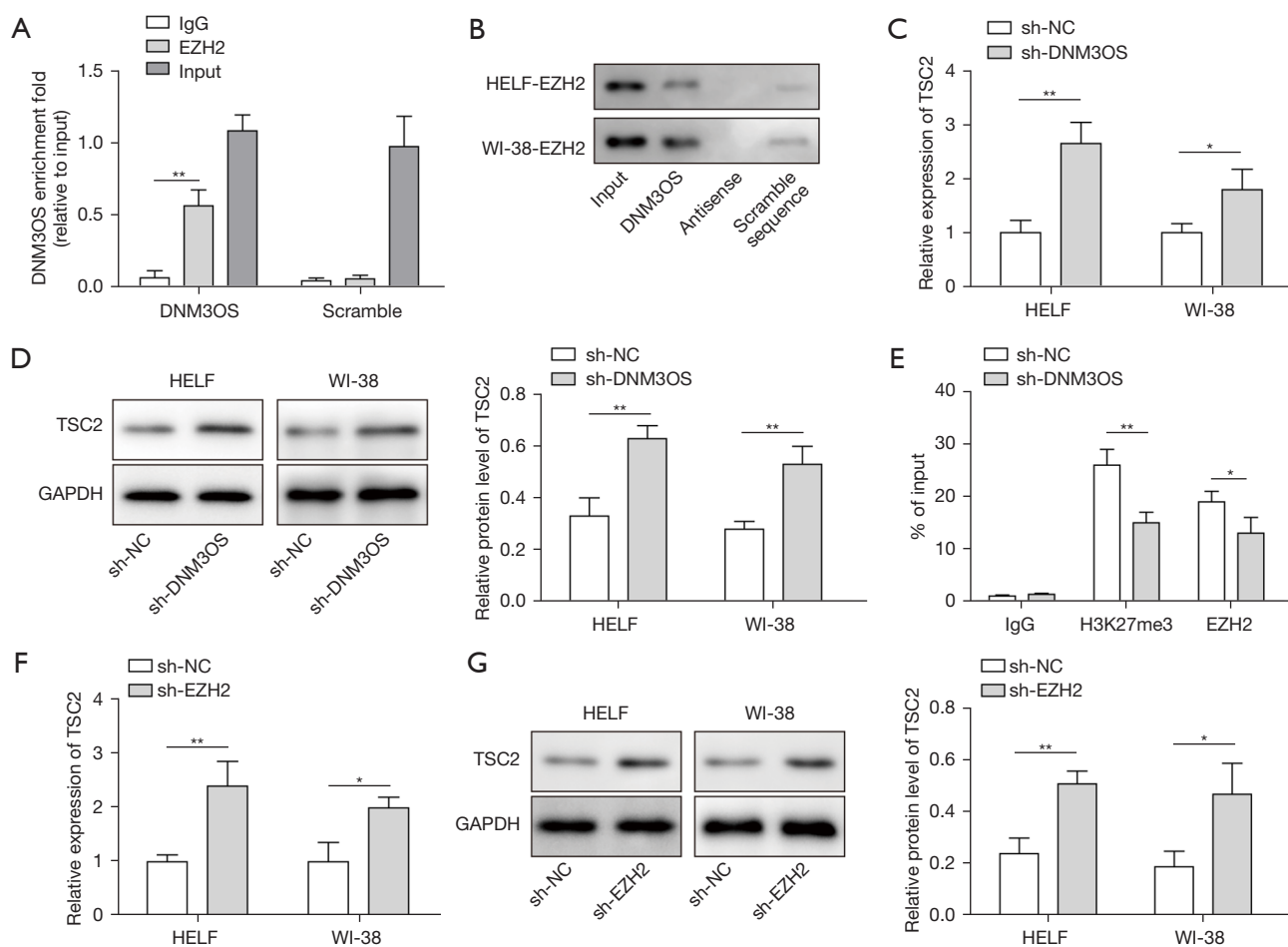
Figure 4 LncRNA *DNM3OS* suppressed the expression of *TSC2* through recruiting EZH2. (A) RIP was performed in HELF and WI-38 cells. *DNM3OS* level in control IgG or EZH2 antibody-enriched fraction was determined by PCR. (B) RNA pull-down assay was performed in HELF and WI-38 cells with *DNM3OS* and antisense RNA. EZH2 level was evaluated by Western blot. (C,D) The mRNA (C) and protein (D) levels of *TSC2* in sh-NC or sh-DNM3OS HELF and WI-38 cells were examined by qRT-PCR and Western blot. (E) ChIP was performed in sh-NC and sh-DNM3OS HELF cells. (F,G) The mRNA (F) and protein (G) levels of *TSC2* in HELF and WI-38 cells transfected with sh-NC or sh-EZH2 were determined by qRT-PCR and western blot analysis. *, P<0.05; **, P<0.01. LncRNA, long noncoding RNA; RIP, RNA immunoprecipitation; HELF, human embryo lung fibroblast; sh-NC, short hairpin RNA negative control; ChIP, chromatin immunoprecipitation; qRT-PCR, quantitative reverse transcription real-time polymerase chain reaction; IgG, immunoglobulin G; GAPDH, glyceraldehyde phosphate dehydrogenase.

LncRNA DNM3OS suppressed TSC2 to promote the expression of fibrosis-related genes in lung fibroblast

To inquire whether *TSC2* is involved in *DNM3OS*-mediated expression of fibrosis-related genes in lung fibroblast, *TSC2* expression was effectively inhibited by *TSC2*-targeting shRNA (*Figure 5A*). TGF-β1-induced cell proliferation was attenuated in sh-DNM3OS cells, while further knockdown of *TSC2* rescued proliferation defect in HELF and WI-38 cells (*Figure 5B*). Reduced migratory ability in

TGF-β1 treated sh-DNM3OS cells was also reversed upon downregulation of *TSC2* (*Figure 5C*). Moreover, *DNM3OS*-dependent induction of *CoL1α1* and *CoL3α1* by TGF-β1 was inhibited in sh-DNM3OS cells but was normalized in cells expressing sh-DNM3OS plus sh-TSC2 (*Figure 5D*). The expression of α-SMA, vimentin, and fibronectin showed similar trends (*Figure 5E*). These data demonstrated that *lncRNA DNM3OS* promoted the expression of fibrosis-related genes in lung fibroblast by suppressing *TSC2* expression.
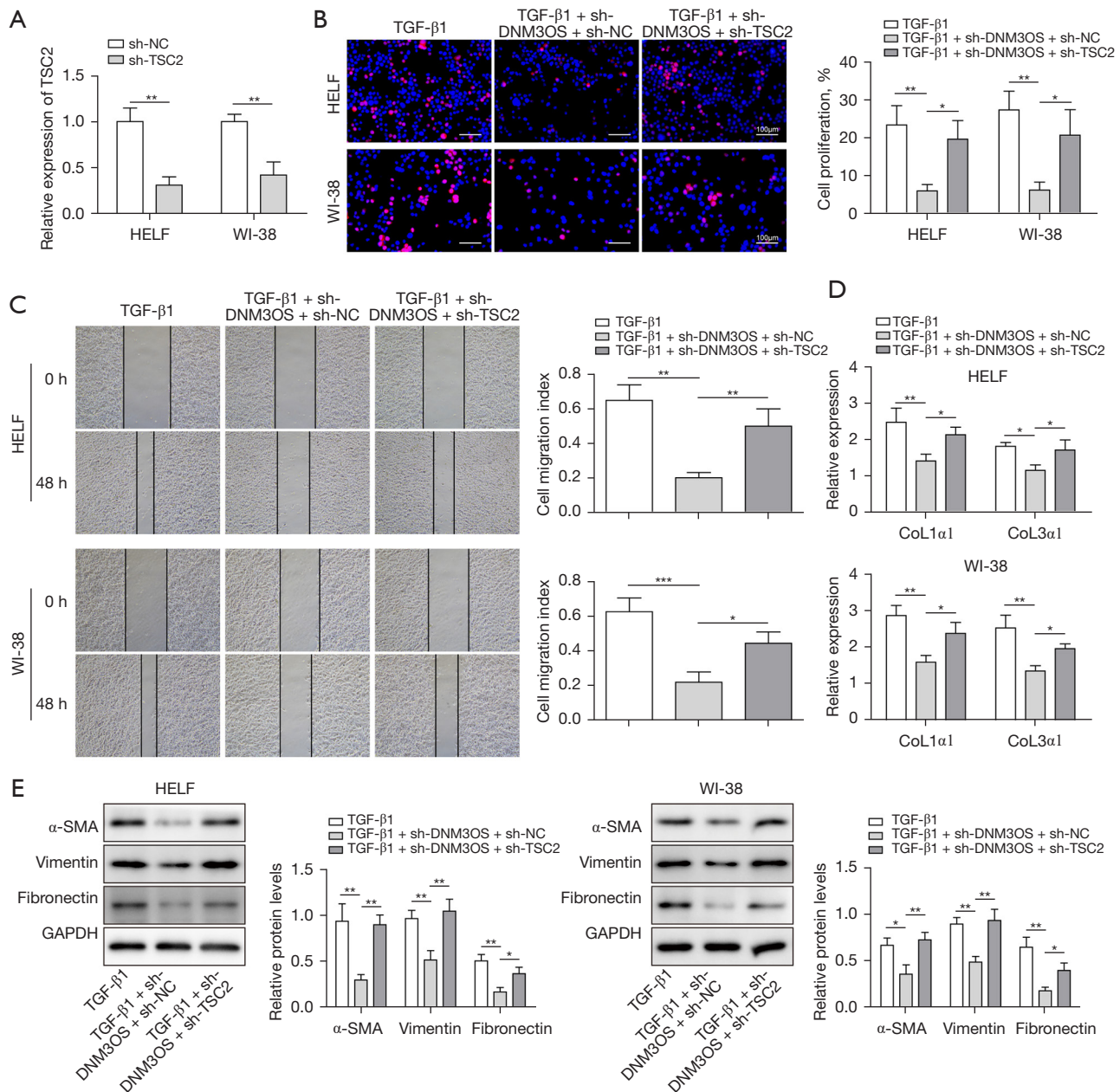
Figure 5 LncRNA *DNM3OS* suppressed *TSC2* to promote the expression of fibrosis-related genes of in lung fibroblast. (A) The level of *TSC2* in HELF and WI-38 cells with sh-NC or sh-TSC2 was determined by qRT-PCR. (B-E) sh-DNM3OS or sh-DNM3OS plus sh-TSC2 were expressed in HELF and WI-38 cells. WT and shRNA expressing lung fibroblasts were treated with control or TGF-β1. The proliferation (B) and migration activity (C) of HELF and WI-38 cells were examined by EdU and wound healing assay, respectively. For EdU assay, the EdU probe was conjugated with a fluorescent dye, and the nucleus was stained by Hoechst 33342 and was examined under a fluorescent microscope. *CoL1α1* and *CoL3α1* levels (D) in HELF and WI-38 cell were evaluated by qRT-PCR. The expressions of α-SMA, vimentin, and fibronectin (E) in HELF and WI-38 cell were evaluated by western blot assay. *, P<0.05; **, P<0.01; ***, P<0.001. LncRNA, long noncoding RNA; HELF, human embryo lung fibroblast; TGF-β1, transforming growth factor beta 1; sh-NC, short hairpin RNA negative control; WT, wide type; qRT-PCR, quantitative reverse transcription real-time polymerase chain reaction; EdU, 5-ethynyl-2'-deoxyuridine; α-SMA, alpha-smooth muscle actin; GAPDH, glyceraldehyde phosphate dehydrogenase.

Discussion

IPF is a chronic, progressive and unrepairable disease with only few available medications to slow down rather than prevent the progression of IPF (27,28). Many adults, particularly elder people, are suffered from IPF and have decreased quality of life worldwide, not to mention the damage and mortality resulted from misdiagnosis and inappropriate treatment (1-3). Due to the poorly understood etiology and pathogenesis of IPF, the potential target for IPF treatment is limited. Herein, we aimed to elucidate the mechanism of *lncRNA DNM3OS*-mediated fibrosis of human embryo lung fibroblast. A pro-fibrotic signaling axis *HOXA5-DNM3OS-TSC2* was revealed in TGF-β1 treated lung fibroblast and targeting this axis showed potential application in anti-fibrosis treatment in the future.

TGF-β signaling is a major contributor for lung fibrosis (29), and many downstream effectors of TGF-β have been identified (30). Recent studies demonstrated that transcription factor *HOXA5* is a critical mesenchymal regulator by regulating Wnt2 signaling (31,32). Moreover, *HOXA5* may also activate TGF-β signaling (33). *HOXA5* also exhibits its transcriptional activity in regulating the expression of *lncRNA0032* (34). A previous study reported that TGF-β upregulates the expression of *DNM3OS* through an unrecognized mechanism (20). We also observed consistent upregulation of *lncRNA DNM3OS* by TGF-β in a dose- and time-dependent manner. We observed downregulation of fibrosis-related genes *CoL1α1* and *CoL1α1* after knockdown of *DNM3OS* in *Figure 3D* and *Figure 5D*. With all the experiments were performed in human embryo lung fibroblast (HELF and Wi-38), our results established the connection between *DNM3OS* and fibrosis. In addition, TGF-β1 is known to be a crucial pro-fibrosis factor in IPF (35,36). IPF patients showed significantly higher production of TGF-β1 compared to healthy controls (37,38). Treatment with TGF-β1 promotes the expression of fibrosis-related genes (39), and Inhibition of TGF-β production prevents IPF progression (40). The analyses of 8 patients with IPF also provided additional verification of the role of *DNM3OS* in pulmonary fibrosis We further exploited a bioinformatics approach which predicted a *HOXA5* binding site in the promoter region of *lncRNA DNM3OS*, and experimentally demonstrated that *HOXA5* regulated the transcription of *lncRNA DNM3OS*. Our study revealed that *HOXA5* promotes the expression of fibrosis-related genes via inducing the transcription of *lncRNA DNM3OS*.

EZH2, a methyltransferase that mediates H3K37 methylation, is involved in TGF-β signaling and related fibrosis (41-43). Our study validated the involvement of EZH2 in TGF-β signaling and further proved that *DNM3OS* may cooperate with EZH2 for the transduction of TGF-β signals. *TSC2* is a suppressor of fibrosis and is epigenetically suppressed by EZH2 (44,45), which is also validated in the current study. LncRNA has shown its versatile functions through various mechanisms including RNA-RNA, RNA-DNA, and RNA-protein interactions (46). As shown in *Figure 5B-5D*, knockdown of *TSC2* partially reversed the effects of shDNM3OS, but could not completely restore to the levels in TGF-β1 treatment, insinuating that there were additional pathways involved in *lncRNA DNM3OS*-mediated lung fibrosis. For instance, a prior study reported the role of *lncRNA DNM3OS* in regulating lung fibrosis through three distinct profibrotic mature miRNAs (20). Furthermore, *lncRNA DNM3OS* modified H3K27 methylation of T-cell lymphoma invasion and metastasis 1 (*TIAM1*) promoter in liver cancer by interacting with lysine demethylase 6B (*KDM6B*) (47). Therefore, *lncRNA DNM3OS*, like other lncRNAs, exerts its functions in many ways. It is difficult for us to exclude the possible involvement of miRNA or other mechanisms in the current study, but we would like to pursue it in the future. Therefore, our study clearly elucidated that induced by TGF-β1-*HOXA5*, *lncRNA DNM3OS* can promote fibrosis of human embryo lung fibroblast by recruiting EZH2 to the promoter region of *TSC2* and epigenetically suppressing the expression of *TSC2*, a suppressor of fibrosis.

Conclusions

Taken together, our study clearly clarified a novel TGF-β signaling axis through which *lncRNA DNM3OS* could aggravate the fibrosis of human embryo lung fibroblast. The *HOXA5-DNM3OS-EZH2-TSC2* axis is essential for fibrosis progression, and targeting this axis holds great potential to treat lung fibrosis.

Acknowledgments

Footnote

Reporting Checklist: The authors have completed the MDAR reporting checklist. Available at https://jtd.amegroups.com/

article/view/10.21037/jtd-23-1145/rc

Data Sharing Statement: Available at https://jtd.amegroups.com/article/view/10.21037/jtd-23-1145/dss

Peer Review File: Available at https://jtd.amegroups.com/article/view/10.21037/jtd-23-1145/prf

Conflicts of Interest: All authors have completed the ICMJE uniform disclosure form (available at https://jtd.amegroups.com/article/view/10.21037/jtd-23-1145/coif). The authors have no conflicts of interest to declare.

Ethical Statement: The authors are accountable for all aspects of the work in ensuring that questions related to the accuracy or integrity of any part of the work are appropriately investigated and resolved. This study was conducted in accordance with the Declaration of Helsinki (as revised in 2013). The study was approved by Taicang TCM Hospital, Affiliated to Nanjing University of Chinese Medicine (No. 2023024). Written informed consent was obtained from each participant in this study.

Open Access Statement: This is an Open Access article distributed in accordance with the Creative Commons Attribution-NonCommercial-NoDerivs 4.0 International License (CC BY-NC-ND 4.0), which permits the non-commercial replication and distribution of the article with the strict proviso that no changes or edits are made and the original work is properly cited (including links to both the formal publication through the relevant DOI and the license). See: https://creativecommons.org/licenses/by-nc-nd/4.0/.

References

1. Lederer DJ, Martinez FJ. Idiopathic Pulmonary Fibrosis. N Engl J Med 2018;378:1811-23.
2. Barratt SL, Creamer A, Hayton C, et al. Idiopathic Pulmonary Fibrosis (IPF): An Overview. J Clin Med 2018;7:201.
3. Samet JM, Coultas D, Raghu G. Idiopathic pulmonary fibrosis: tracking the true occurrence is challenging. Eur Respir J 2015;46:604-6.
4. Selman M, Pardo A. Revealing the pathogenic and aging-related mechanisms of the enigmatic idiopathic pulmonary fibrosis. an integral model. Am J Respir Crit Care Med 2014;189:1161-72.
5. Alder JK, Chen JJ, Lancaster L, et al. Short telomeres are a risk factor for idiopathic pulmonary fibrosis. Proc Natl Acad Sci U S A 2008;105:13051-6.
6. Misharin AV, Morales-Nebreda L, Reyfman PA, et al. Monocyte-derived alveolar macrophages drive lung fibrosis and persist in the lung over the life span. J Exp Med 2017;214:2387-404.
7. Raghu G, Rochwerg B, Zhang Y, et al. An Official ATS/ERS/JRS/ALAT Clinical Practice Guideline: Treatment of Idiopathic Pulmonary Fibrosis. An Update of the 2011 Clinical Practice Guideline. Am J Respir Crit Care Med 2015;192:e3-19.
8. Hafner A, Boettiger A. The spatial organization of transcriptional control. Nat Rev Genet 2023;24:53-68.
9. Lin S, Zhang R, Xu L, et al. LncRNA Hoxaas3 promotes lung fibroblast activation and fibrosis by targeting miR-450b-5p to regulate Runx1. Cell Death Dis 2020;11:706.
10. Mümmler C, Burgy O, Hermann S, et al. Cell-specific expression of runt-related transcription factor 2 contributes to pulmonary fibrosis. FASEB J 2018;32:703-16.
11. Chen L, Yang Y, Peng X, et al. Transcription factor YY1 inhibits the expression of THY1 to promote interstitial pulmonary fibrosis by activating the HSF1/miR-214 axis. Aging (Albany NY) 2020;12:8339-51.
12. Huang C, Liang C, Tong J, et al. Soluble E-cadherin participates in BLM-induced pulmonary fibrosis by promoting EMT and lung fibroblast migration. Environ Toxicol 2024;39:435-43.
13. Espindola MS, Habiel DM, Narayanan R, et al. Targeting of TAM Receptors Ameliorates Fibrotic Mechanisms in Idiopathic Pulmonary Fibrosis. Am J Respir Crit Care Med 2018;197:1443-56.
14. Fujino N, Kubo H, Maciewicz RA. Phenotypic screening identifies Axl kinase as a negative regulator of an alveolar epithelial cell phenotype. Lab Invest 2017;97:1047-62.
15. Nojima T, Proudfoot NJ. Mechanisms of lncRNA biogenesis as revealed by nascent transcriptomics. Nat Rev Mol Cell Biol 2022;23:389-406.
16. Herman AB, Tsitsipatis D, Gorospe M. Integrated lncRNA function upon genomic and epigenomic regulation. Mol Cell 2022;82:2252-66.
17. Tang PC, Zhang YY, Li JS, et al. LncRNA-Dependent Mechanisms of Transforming Growth Factor-β: From Tissue Fibrosis to Cancer Progression. Noncoding RNA 2022;8:36.
18. Chen T, Shi Z, Zhao Y, et al. LncRNA Airn maintains LSEC differentiation to alleviate liver fibrosis via the KLF2-eNOS-sGC pathway. BMC Med 2022;20:335.

19. Qian W, Cai X, Qian Q, et al. lncRNA ZEB1-AS1 promotes pulmonary fibrosis through ZEB1-mediated epithelial-mesenchymal transition by competitively binding miR-141-3p. Cell Death Dis 2019;10:129.

20. Savary G, Dewaeles E, Diazzi S, et al. The Long Noncoding RNA DNM3OS Is a Reservoir of FibromiRs with Major Functions in Lung Fibroblast Response to TGF-β and Pulmonary Fibrosis. Am J Respir Crit Care Med 2019;200:184-98.

21. Savary G, Buscot M, Dewaeles E, et al. Targeting the DNM3OS / miR-199a~214 cluster for the treatment of fibroproliferative diseases. bioRxiv preprint. 2018. doi: 10.1101/242040.

22. Raghu G, Collard HR, Egan JJ, et al. An official ATS/ERS/JRS/ALAT statement: idiopathic pulmonary fibrosis: evidence-based guidelines for diagnosis and management. Am J Respir Crit Care Med 2011;183:788-824.

23. Walsh SL, Sverzellati N, Devaraj A, et al. Connective tissue disease related fibrotic lung disease: high resolution computed tomographic and pulmonary function indices as prognostic determinants. Thorax 2014;69:216-22.

24. Gagliardi M, Matarazzo MR. RIP: RNA Immunoprecipitation. Methods Mol Biol 2016;1480:73-86.

25. Bai Q, Bai Z, Sun L. Detection of RNA-binding Proteins by In Vitro RNA Pull-down in Adipocyte Culture. J Vis Exp 2016.

26. Xiong F, Liu W, Wang X, et al. HOXA5 inhibits the proliferation of extrahepatic cholangiocarcinoma cells by enhancing MXD1 expression and activating the p53 pathway. Cell Death Dis 2022;13:829.

27. Thong L, McElduff EJ, Henry MT. Trials and Treatments: An Update on Pharmacotherapy for Idiopathic Pulmonary Fibrosis. Life (Basel) 2023;13:486.

28. Trachalaki A, Sultana N, Wells AU. An update on current and emerging drug treatments for idiopathic pulmonary fibrosis. Expert Opin Pharmacother 2023;24:1125-42.

29. Ren LL, Li XJ, Duan TT, et al. Transforming growth factor-β signaling: From tissue fibrosis to therapeutic opportunities. Chem Biol Interact 2023;369:110289.

30. Peng D, Fu M, Wang M, et al. Targeting TGF-β signal transduction for fibrosis and cancer therapy. Mol Cancer 2022;21:104.

31. Goss AM, Tian Y, Cheng L, et al. Wnt2 signaling is necessary and sufficient to activate the airway smooth muscle program in the lung by regulating myocardin/Mrtf-B and Fgf10 expression. Dev Biol 2011;356:541-52.

32. Hrycaj SM, Dye BR, Baker NC, et al. Hox5 Genes Regulate the Wnt2/2b-Bmp4-Signaling Axis during Lung Development. Cell Rep 2015;12:903-12.

33. Zhang Y, Da Q, Cao S, et al. HINT1 (Histidine Triad Nucleotide-Binding Protein 1) Attenuates Cardiac Hypertrophy Via Suppressing HOXA5 (Homeobox A5) Expression. Circulation 2021;144:638-54.

34. Zhu Q, Lv T, Wu Y, et al. Long non-coding RNA 00312 regulated by HOXA5 inhibits tumour proliferation and promotes apoptosis in Non-small cell lung cancer. J Cell Mol Med 2017;21:2184-98.

35. Ye Z, Hu Y. TGF-β1: Gentlemanly orchestrator in idiopathic pulmonary fibrosis (Review). Int J Mol Med 2021;48:132.

36. Chong DLW, Mikolasch TA, Sahota J, et al. Investigating the role of platelets and platelet-derived transforming growth factor-β in idiopathic pulmonary fibrosis. Am J Physiol Lung Cell Mol Physiol 2023;325:L487-99.

37. Larson-Casey JL, Deshane JS, Ryan AJ, et al. Macrophage Akt1 Kinase-Mediated Mitophagy Modulates Apoptosis Resistance and Pulmonary Fibrosis. Immunity 2016;44:582-96.

38. Yu X, Buttgereit A, Lelios I, et al. The Cytokine TGF-β Promotes the Development and Homeostasis of Alveolar Macrophages. Immunity 2017;47:903-912.e4.

39. Wu M, Wang Z, Shi X, et al. TGFβ1-RCN3-TGFBR1 loop facilitates pulmonary fibrosis by orchestrating fibroblast activation. Respir Res 2023;24:222.

40. He J, Du Y, Li G, et al. Myeloid Fbxw7 Prevents Pulmonary Fibrosis by Suppressing TGF-β Production. Front Immunol 2021;12:760138.

41. Zhang L, Qu J, Qi Y, et al. EZH2 engages TGFβ signaling to promote breast cancer bone metastasis via integrin β1-FAK activation. Nat Commun 2022;13:2543.

42. Peng Y, Liao K, Tan F, et al. Suppression of EZH2 inhibits TGF-β1-induced EMT in human retinal pigment epithelial cells. Exp Eye Res 2022;222:109158.

43. Zhang Q, Wu YX, Yu XQ, et al. EZH2 serves as a promising therapeutic target for fibrosis. Bioorg Chem 2023;137:106578.

44. Kaneko-Tarui T, Commandeur AE, Patterson AL, et al. Hyperplasia and fibrosis in mice with conditional loss of the TSC2 tumor suppressor in Müllerian duct mesenchyme-derived myometria. Mol Hum Reprod 2014;20:1126-34.

45. Wei FZ, Cao Z, Wang X, et al. Epigenetic regulation of autophagy by the methyltransferase EZH2 through an MTOR-dependent pathway. Autophagy 2015;11:2309-22.

46. Mattick JS, Amaral PP, Carninci P, et al. Long non-coding RNAs: definitions, functions, challenges and

recommendations. Nat Rev Mol Cell Biol 2023;24:430-47.

47. Wang W, Wang Q, Huang DB, et al. Tumor-associated mesenchymal stem cells promote hepatocellular carcinoma metastasis via a DNM3OS/KDM6B/TIAM1 axis. Cancer Lett 2021;503:19-31.
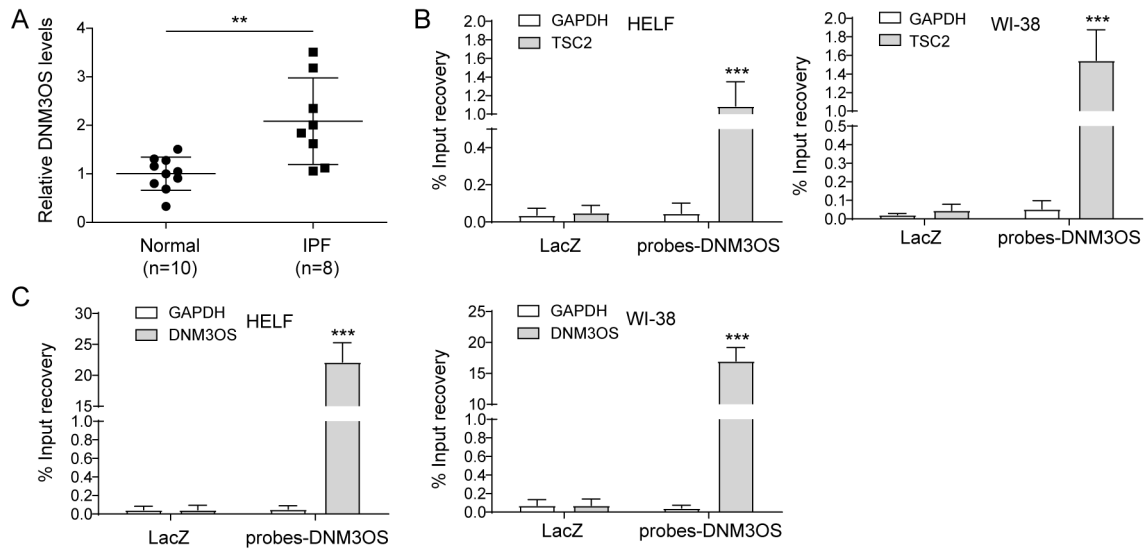
Figure S1 LncRNA *DNM3OS* was upregulated in IPF and could bind to the promoter of *TSC2*. (A) the levels of *lncRNA DNM3OS* in the blood of healthy controls (n=10) and IPF patients (n=8) were evaluated by qRT-PCR. ChIRP was performed: (B) *DNM3OS* bound to the promoter of *TSC2* was determined by qPCR. (C) The specific binding of *DNM3OS* with its probes was verified using qRT-PCR. **, P<0.01; ***, P<0.001.